

Supporting Information

Skruzny et al. 10.1073/pnas.1207011109

SI Materials and Methods

Fluorescence Recovery After Photobleaching. The fluorescence recovery after photobleaching (FRAP) experiments were done with a custom-built set-up that focuses a 488-nm laser beam at the sample plane. The diameter of the bleach spot was $\sim 0.5 \mu\text{m}$ and thus covered the endocytic site completely. The acquired image series were background subtracted and normalized. The centroid position of the bleached endocytic site was determined with a custom-written segmentation algorithm in MATLAB (Mathworks), and the fluorescence recovery within a circle with a radius of four pixels around the centroid position was calculated. The recovery curves of several individual experiments were aligned to the bleaching time, and the average recovery curve was calculated.

Preparation of Lipid Solutions. Lipid mixtures [96 mol% dioleoylphosphatidylcholine (DOPC) and 4 mol% phosphatidylinositol (4,5)-bisphosphate [PI(4,5)P₂] or 92 mol% DOPC and 8 mol% dioleoylphosphatidylserine (DOPS) (Avanti Polar Lipids)] were prepared to a final concentration of 2.5 mM total lipid. Lipid solutions were mixed, and the organic solvent was evaporated under an argon stream followed by 30 min in vacuum. Lipids were hydrated by agitation with 20 mM Hepes (pH 7.5) and 100 mM KCl for 90 min at 65 °C followed by brief sonication and three snap-freeze/thaw cycles in liquid nitrogen. Liposomes were prepared by extrusion through 100- or 400-nm polycarbonate filters using an Avanti Mini-Extruder according to the manufacturer's instructions.

Protein Expression and Purification. Recombinant proteins were expressed as 6xHis-GST-fusions from pETM30 plasmid in *Escherichia coli* BL21-CodonPlus cells (Stratagene). The cell culture was grown in LB medium at 37 °C to OD₆₀₀ 0.6–0.8, and the expression of the protein was induced by 0.3–0.5 mM isopropylthio- β -galactoside (IPTG) followed by 3-h incubation at 25 °C or 28 °C. Cells were lysed by sonication in running buffer [50 mM Hepes (pH 7.5), 100 mM KCl, 20 mM imidazole, 1 mM β -mercaptoethanol] with Complete EDTA-free protease inhibitors mix (Roche). The protein was bound on a Ni-NTA column (QIAGEN), washed with running buffer, and eluted with a linear gradient of 20–300 mM imidazole in running buffer. The 6xHis-GST moiety

of the protein was cleaved by His-TEV protease, and the protein was dialyzed against 20 mM Hepes (pH 7.5), 100 mM KCl, and 1 mM DTT overnight at 4 °C. The protein solution then was passed through a Ni-NTA column to remove uncleaved protein, His-GST, and His-TEV and was purified further by ion exchange using a HiTrap Q column (GE Healthcare). Alternatively, cells were lysed by microfluidizer (Microfluidics) in a mix of PBS, 250 mM NaCl, and 5 mM DTT, with protease inhibitors. The protein was bound on a GSTrap HP column or glutathione beads (GE Healthcare), washed with 10 \times column volumes (CV) of PBS, 250 mM NaCl, and 1 mM DTT, and eluted by 3 \times CV of 100 mM Tris-HCl (pH 8.0), 150 mM KCl, and 15 mM glutathione. The 6xHis-GST moiety of the protein was cleaved by His-TEV protease, and the protein was dialyzed against 50 mM Hepes (pH 7.5); 150 mM KCl, 20 mM imidazole, and 2 mM β -mercaptoethanol overnight at 4 °C. A Ni-NTA column then was used to remove impurities as above. The final eluted fractions with pure protein (as assessed by SDS/PAGE and Coomassie staining) were collected, concentrated, and dialyzed against the desired buffer. Concentrated pure protein was snap-frozen in liquid nitrogen and stored at $-80 \text{ }^\circ\text{C}$ before use.

Actin Cosedimentation Assays. The actin cosedimentation assays were performed according to the manufacturer's protocols (Cytoskeleton). Briefly, 1–2 mg/mL of human nonmuscle or muscle actin (Cytoskeleton) was polymerized for 1 h at 25 °C and then mixed with the protein (precleared by centrifugation at 150,000 $\times g$ for 1 h at 4 °C) to reach a final concentration of 5 μM for the protein and 0.15–45 μM for F-actin (50 μL total volume). Alternatively, to check for possible capping or G-actin sequestering activity of the protein, the actin was polymerized in the presence of protein. After 30 min incubation at 25 °C, F-actin and an associated protein were pelleted by centrifugation at 150,000 $\times g$ for 1.5 h at 25 °C. The supernatant and pellet were brought to equal volumes of SDS/PAGE loading buffer, and their protein content was analyzed by SDS/PAGE using 4–12% Bis-Tris gel in MES buffer (Invitrogen) and Brilliant Blue G-Colloidal staining (Sigma). The amounts of protein pelleted by F-actin and of the unbound protein in the supernatant were quantified densitometrically using Kodak Image Station 4000MM PRO and ImageJ software.

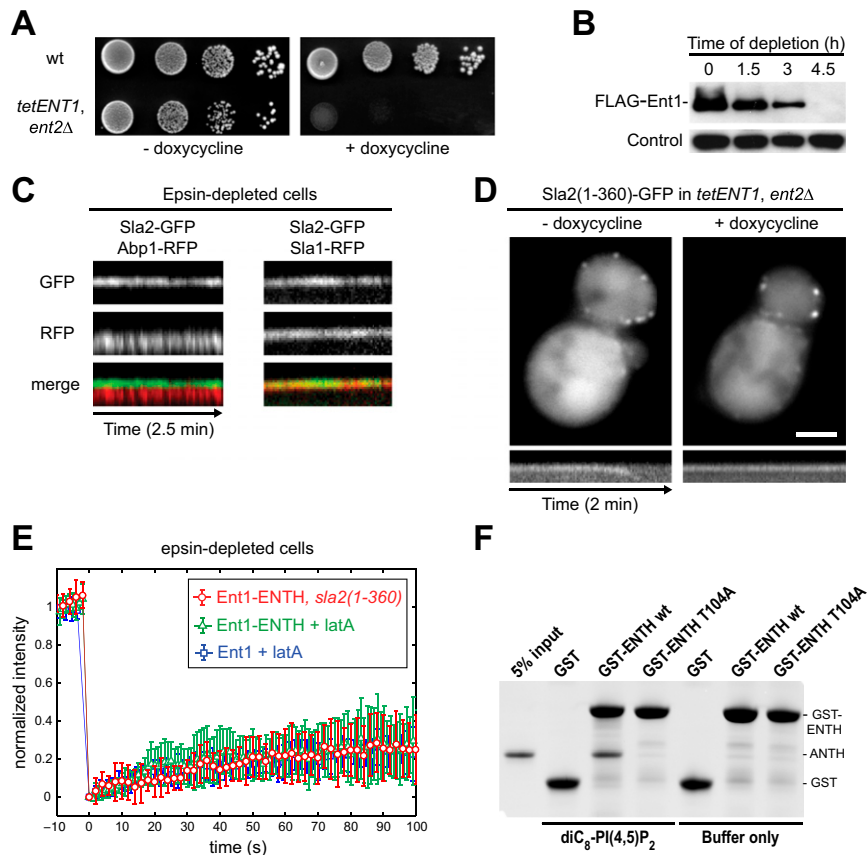


Fig. S1. Behavior of Sla2-GFP and Sla2(1–360)-GFP at endocytic sites of epsin-depleted cells. (A) Growth phenotype of epsin-depleted cells. Wild-type (wt) and epsin-depleted (*tetENT1, ent2Δ*) strains were spotted in 10-fold serial dilutions on yeast extract/peptone/dextrose (YPD) plates or on YPD plates containing 25 $\mu\text{g}/\text{mL}$ doxycycline and were incubated for 2.5 d at 30 $^{\circ}\text{C}$. (B) Time course of Ent1 depletion. Whole-cell lysates of the *tetENT1, ent2Δ* strain were prepared at the indicated time points after incubation with doxycycline. Expression of FLAG-Ent1 protein was analyzed by immunoblotting with anti-FLAG antibody. The detection of Arc1 protein by anti-Arc1 antibody was used as a loading control. (C) Sla2 colocalizes with the endocytic coat in epsin-depleted cells. Kymographs of Sla2-GFP and Abp1-RFP or Sla2-GFP and Sla1-RFP at endocytic patches of epsin-depleted cells are shown as separate channels and merged images. All kymographs are oriented with the cell exterior at the top. (Upper) Localization of Sla2(1–360)-GFP before (– doxycycline) and after (+ doxycycline) epsin depletion. (Scale bar: 2 μm .) (Lower) Kymographs of Sla2(1–360)-GFP at endocytic patches. (E) FRAP of Ent1-ENTH-GFP at endocytic sites in epsin-depleted *sla2(1–360)* cells. The Ent1-GFP FRAP in latrunculin A (latA)-treated wild-type cells (from Fig. 1C) and Ent1-ENTH-GFP FRAP in latA-treated epsin-depleted *sla2(1–360)* cells (from Fig. 2C) are shown for comparison. The recovery curves represent the mean \pm SD ($n = 7$ –12 separate measurements). (F) ANTH binds GST-ENTH in the presence of the soluble lipid ligand dioctanoyl-PI(4,5)P₂ [diC₈-PI(4,5)P₂]. Glutathione beads with GST-ENTH, GST-ENTH T104A, or GST alone were incubated with an equimolar amount of ANTH protein in the presence or absence of diC₈-PI(4,5)P₂ at 25 $^{\circ}\text{C}$. Beads with bound proteins were analyzed by SDS/PAGE and Coomassie staining.

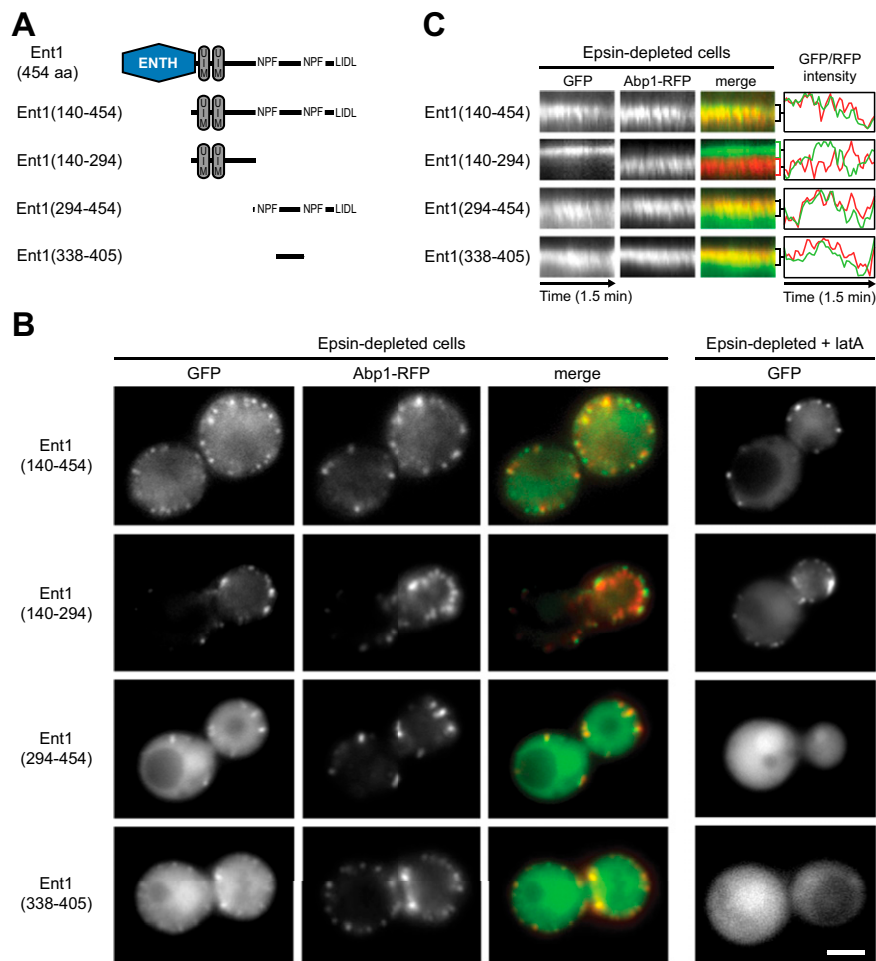


Fig. S2. Characterization of the Ent1 actin cytoskeleton-binding (ACB) domain. (A) A schematic of Ent1 C-terminal constructs. Protein domains and linear motifs for binding EH-domain proteins (NPF) and clathrin (LIDL) are shown. (B) Localization of Ent1 C-terminal fragments fused to GFP and Abp1-RFP at endocytic sites of epsin-depleted cells with or without latA treatment. Separate channels and merged images are shown for untreated cells; the GFP channel is shown for latA-treated cells. (Scale bar: 2 μ m.) (C) Kymographs and corresponding fluorescence intensity profiles of GFP-tagged Ent1 C-terminal fragments and Abp1-RFP at endocytic patches of epsin-depleted cells. Separate channels, merged images, and normalized GFP/RFP intensity profiles from the indicated area of cell cortex are shown. All kymographs are oriented with the cell exterior at the top.

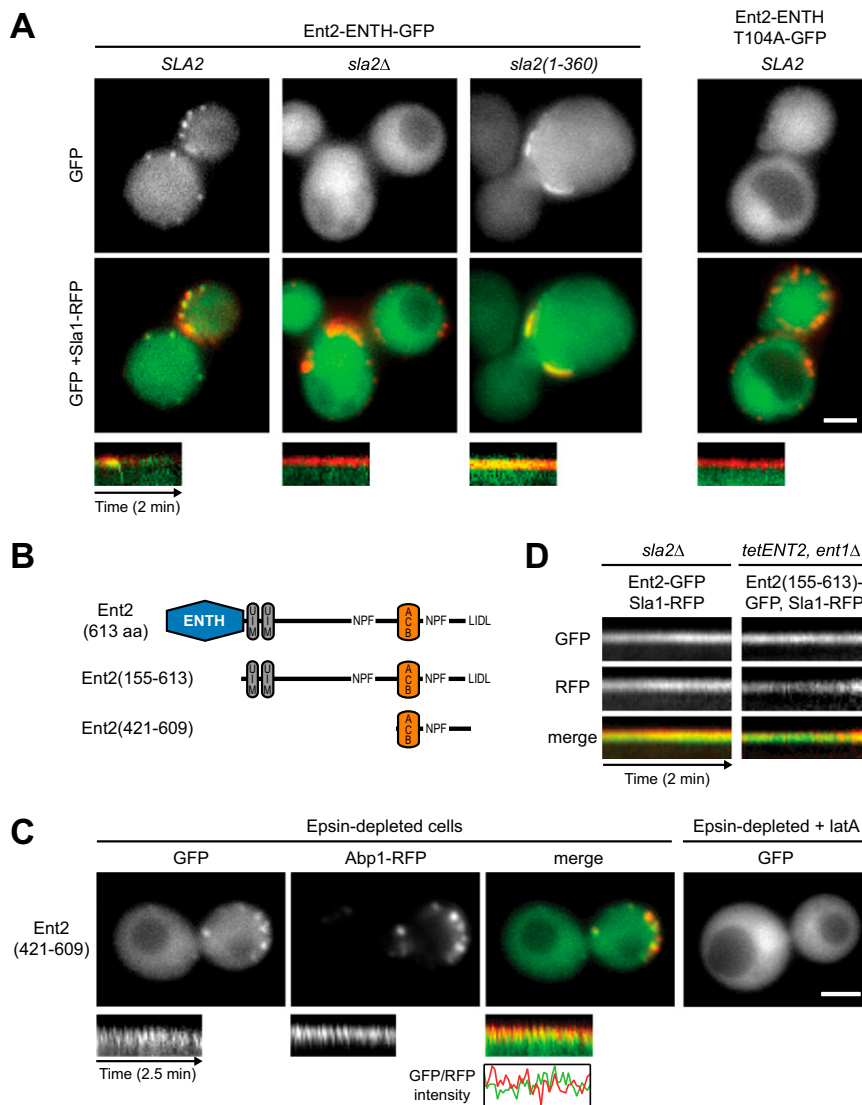


Fig. S3. Characterization of Ent2 ENTH and ACB domains. (A) (Upper) Localization of Ent2-ENTH-GFP and Ent2-ENTH(T104A)-GFP together with Sla1-RFP in epsin-depleted cells in the presence or absence of Sla2. GFP and merged images are shown. (Lower) Kymographs of Ent2-ENTH-GFP, Ent2-ENTH(T104A)-GFP, and Sla1-RFP at endocytic patches. (B) A schematic of Ent2 C-terminal constructs. Protein domains and linear motifs for binding EH-domain proteins (NPF) and clathrin (LIDL) are shown. (C) (Upper) Localization of Ent2(421–609)-GFP and Abp1-RFP at endocytic sites of epsin-depleted cells with or without latA treatment. Separate channels and merged images are shown for untreated cells; the GFP channel is shown for latA-treated cells. (Lower) Kymographs and corresponding normalized intensity profiles of Ent2(421–609)-GFP and Abp1-RFP at a single endocytic patch. All kymographs are oriented with the cell exterior at the top. (D) Kymographs of Sla1-RFP together with Ent2-GFP or Ent2(155–613)-GFP at a single endocytic patch of *sla2Δ* and epsin-depleted cells (*tetENT2, ent1Δ*) are shown as separate channels and merged images. (Scale bars: 2 μ m in A and C.)

Table S1. Yeast strains used in this study

Strain	Genotype
MKY0140	MATa, <i>his3Δ200</i> , <i>leu2-3,112</i> , <i>ura3-52</i> , <i>lys2-801</i> , <i>SLA1-EGFP::HIS3MX6</i>
MKY0154	MATa, <i>his3Δ200</i> , <i>leu2-3,112</i> , <i>ura3-52</i> , <i>lys2-801</i> , <i>ABP1-mCherry::kanMX4</i>
MKY0255	MATa, <i>his3Δ200</i> , <i>leu2-3,112</i> , <i>ura3-52</i> , <i>lys2-801</i> , <i>YAP1802-EGFP::HIS3MX6</i>
MKY0677	MATα, <i>his3Δ200</i> , <i>leu2-3,112</i> , <i>ura3-52</i> , <i>lys2-801</i> , <i>PAN1-EGFP::HIS3MX6</i>
MKY0822	MATa, <i>his3Δ200</i> , <i>leu2-3,112</i> , <i>ura3-52</i> , <i>lys2-801</i> , <i>SLA1-EGFP::HIS3MX6</i> , <i>ABP1-mCherry::kanMX4</i>
MKY0901	MATa, <i>his3Δ200</i> , <i>leu2-3,112</i> , <i>ura3-52</i> , <i>lys2-801</i> , <i>ENT1-EGFP::HIS3MX6</i>
MKY0903	MATa, <i>his3Δ200</i> , <i>leu2-3,112</i> , <i>ura3-52</i> , <i>lys2-801</i> , <i>ENT2-EGFP::HIS3MX6</i>
MKY0922	MATa, <i>his3Δ200</i> , <i>leu2-3,112</i> , <i>ura3-52</i> , <i>lys2-801</i> , <i>sla2:natNT2</i> , <i>SLA1-EGFP::HIS3MX6</i>
MKY0927	MATα, <i>his3Δ200</i> , <i>leu2-3,112</i> , <i>ura3-52</i> , <i>lys2-801</i> , <i>sla2:natNT2</i> , <i>PAN1-EGFP::HIS3MX6</i>
MKY0930	MATa, <i>his3Δ200</i> , <i>leu2-3,112</i> , <i>ura3-52</i> , <i>lys2-801</i> , <i>sla2:natNT2</i> , <i>YAP1802-EGFP::HIS3MX6</i>
MKY0962	MATa, <i>his3Δ200</i> , <i>leu2-3,112</i> , <i>ura3-52</i> , <i>lys2-801</i> , <i>sla2:natNT2</i> , <i>ENT1-EGFP::HIS3MX6</i>
MKY0964	MATa, <i>his3Δ200</i> , <i>leu2-3,112</i> , <i>ura3-52</i> , <i>lys2-801</i> , <i>sla2:natNT2</i> , <i>ENT2-EGFP::HIS3MX6</i>
MKY1060	MATa, <i>his3Δ200</i> , <i>leu2-3,112</i> , <i>ura3-52</i> , <i>lys2-801</i> , <i>sla2:natNT2</i> , <i>END3-EGFP::HIS3MX6</i>
MKY1096	MATaα, <i>his3Δ200</i> , <i>ura3-52</i> , <i>lys2-801</i> , <i>sla2(1-360)::HIS3MX6</i> , <i>ENT1-EGFP::HIS3MX6</i> , <i>SLA1-mCherry::kanMX4</i>
MKY1099	MATα, <i>his3Δ200</i> , <i>ura3-52</i> , <i>lys2-801</i> , <i>ent1::hphNT1</i> , <i>tetO₂(ENT2)::HIS3MX6</i> , <i>tetR':LEU2</i> , <i>SLA2-EGFP::natNT2</i>
MKY1101	MATα, <i>his3Δ200</i> , <i>ura3-52</i> , <i>lys2-801</i> , <i>ent2::hphNT1</i> , <i>tetO₂(ENT1)::kanMX4</i> , <i>tetR':LEU2</i> , <i>SLA1-EGFP::HIS3MX6</i> , <i>ABP1-mCherry::kanMX4</i>
MKY1119	MATα, <i>his3Δ200</i> , <i>ura3-52</i> , <i>lys2-801</i> , <i>ent2::hphNT1</i> , <i>tetO₂(ENT1)::kanMX4</i> , <i>tetR':LEU2</i>
MKY1142	MATα, <i>his3Δ200</i> , <i>ura3-52</i> , <i>lys2-801</i> , <i>ent1::hphNT1</i> , <i>tetO₂(ENT2)::HIS3MX6</i> , <i>tetR':LEU2</i> , <i>sla2(1-360)-EGFP::HIS3MX6</i>
MKY1145	MATα, <i>his3Δ200</i> , <i>ura3-52</i> , <i>lys2-801</i> , <i>ent1::hphNT1</i> , <i>tetO₂(ENT2)::HIS3MX6</i> , <i>tetR':LEU2</i>
MKY1146	MATaα, <i>his3Δ200</i> , <i>ura3-52</i> , <i>lys2-801</i> , <i>ent1::hphNT1</i> , <i>tetO₂(ENT2)::HIS3MX6</i> , <i>tetR':LEU2</i> , <i>SLA1-mCherry::kanMX4</i>
MKY1148	MATaα, <i>his3Δ200</i> , <i>ura3-52</i> , <i>lys2-801</i> , <i>ent1::hphNT1</i> , <i>tetO₂(ENT2)::HIS3MX6</i> , <i>tetR':LEU2</i> , <i>SLA1-EGFP::kanMX4</i> , <i>ABP1-mCherry::kanMX4</i>
MKY1172	MATα, <i>his3Δ200</i> , <i>ura3-52</i> , <i>lys2-801</i> , <i>ENT1-EGFP::HIS3MX6</i> , <i>sla2ΔTHATCH::natNT2</i>
MKY1195	MATa, <i>his3Δ200</i> , <i>leu2-3,112</i> , <i>ura3-52</i> , <i>lys2-801</i> , <i>sla2:natNT2</i> , <i>SLA1-EGFP::HIS3MX6</i> , <i>ABP1-mCherry::kanMX4</i>
MKY1198	MATa, <i>his3Δ200</i> , <i>leu2-3,112</i> , <i>ura3-52</i> , <i>lys2-801</i> , <i>END3-EGFP::HIS3MX6</i>
MKY1370	MATa, <i>his3Δ200</i> , <i>leu2-3,112</i> , <i>ura3-52</i> , <i>lys2-801</i> , <i>SYPI-EGFP::HIS3MX6</i>
MKY1394	MATa, <i>his3Δ200</i> , <i>leu2-3,112</i> , <i>ura3-52</i> , <i>lys2-801</i> , <i>sla2:natNT2</i> , <i>SYPI-EGFP::HIS3MX6</i>
MKY1828	MATa, <i>his3Δ200</i> , <i>leu2-3,112</i> , <i>ura3-52</i> , <i>lys2-801</i> , <i>SLA2-EGFP::natNT2</i>
MKY1829	MATa, <i>his3Δ200</i> , <i>leu2-3,112</i> , <i>ura3-52</i> , <i>lys2-801</i> , <i>sla2:natNT2</i> , <i>ENT1-EGFP::HIS3MX6</i> , <i>SLA1-mCherry::kanMX4</i>
MKY1830	MATaα, <i>his3Δ200</i> , <i>leu2-3,112</i> , <i>ura3-52</i> , <i>lys2-801</i> , <i>sla2:natNT2</i> , <i>ENT1-EGFP::HIS3MX6</i> , <i>ABP1-mCherry::kanMX4</i>
MKY1831	MATaα, <i>his3Δ200</i> , <i>ura3-52</i> , <i>lys2-801</i> , <i>ent2::hphNT1</i> , <i>tetO₂(ENT1)::kanMX4</i> , <i>tetR':LEU2</i> , <i>SLA1-EGFP::HIS3MX6</i> , <i>ABP1-mCherry::kanMX4</i>
MKY1833	MATaα, <i>his3Δ200</i> , <i>ura3-52</i> , <i>lys2-801</i> , <i>ent1::KIURA3</i> , <i>tetO₂(ENT2)::HIS3MX6</i> , <i>tetR':LEU2</i> , <i>EDE1-EGFP::HIS3MX6</i> , <i>SLA1-mCherry::kanMX4</i>
MKY1834	MATaα, <i>his3Δ200</i> , <i>ura3-52</i> , <i>lys2-801</i> , <i>ent1::KIURA3</i> , <i>tetO₂(ENT2)::HIS3MX6</i> , <i>tetR':LEU2</i> , <i>SLA2-EGFP::natNT2</i> , <i>SLA1-mCherry::kanMX4</i>
MKY1837	MATaα, <i>his3Δ200</i> , <i>ura3-52</i> , <i>lys2-801</i> , <i>ent1::KIURA3</i> , <i>tetO₂(ENT2)::HIS3MX6</i> , <i>tetR':LEU2</i> , <i>PAN1-EGFP::HIS3MX6</i> , <i>ABP1-mCherry::kanMX4</i>
MKY1838	MATaα, <i>his3Δ200</i> , <i>ura3-52</i> , <i>lys2-801</i> , <i>ent2::hphNT1</i> , <i>sla2:natNT2</i> , <i>tetO₂(ENT1)::kanMX4</i> , <i>tetR':LEU2</i> , <i>SLA1-mCherry::kanMX4</i>
MKY1839	MATaα, <i>his3Δ200</i> , <i>ura3-52</i> , <i>lys2-801</i> , <i>ent1::hphNT1</i> , <i>sla2:natNT2</i> , <i>tetO₂(ENT2)::HIS3MX6</i> , <i>tetR':LEU2</i> , <i>SLA1-mCherry::kanMX4</i>

Table S1. Cont.

Strain	Genotype
MKY1840	MATa α , <i>his3Δ200</i> , <i>ura3-52</i> , <i>lys2-801</i> , <i>ent2::hphNT1</i> , <i>tetO₂(ENT1)::HIS3MX6</i> , <i>sla2(1-360)::HIS3MX6</i> , <i>SLA1-mCherry::kanMX4</i>
MKY1841	MATa α , <i>his3Δ200</i> , <i>ura3-52</i> , <i>lys2-801</i> , <i>ent2::hphNT1</i> , <i>tetO₂(ENT1)::HIS3MX6</i> , <i>tetR::LEU2</i> , <i>ABP1-mCherry::kanMX4</i>
MKY1842	MATa α , <i>his3Δ200</i> , <i>ura3-52</i> , <i>lys2-801</i> , <i>ent1::hphNT1</i> , <i>tetO₂(ENT2)::kanMX4</i> , <i>tetR::LEU2</i> , <i>ABP1-mCherry::kanMX4</i>
MKY1843	MATa α , <i>his3Δ200</i> , <i>ura3-52</i> , <i>lys2-801</i> , <i>ENT1-EGFP::HIS3MX6</i> , <i>ABP1-mCherry::kanMX4</i>
MKY1844	MATa α , <i>his3Δ200</i> , <i>ura3-52</i> , <i>lys2-801</i> , <i>sla2ΔTHATCH::natNT2</i> , <i>ENT1-EGFP::HIS3MX6</i> , <i>ABP1-mCherry::kanMX4</i>
MKY1845	MATa α , <i>his3Δ200</i> , <i>ura3-52</i> , <i>lys2-801</i> , <i>ent1ΔACB(Δ amino acids 294–450)-EGFP::HIS3MX6</i> , <i>ABP1-mCherry::kanMX4</i>
MKY1846	MATa α , <i>his3Δ200</i> , <i>ura3-52</i> , <i>lys2-801</i> , <i>ent1ΔACB(Δ amino acids 294–450)-EGFP::HIS3MX6</i> , <i>sla2ΔTHATCH::natNT2</i> , <i>ABP1-mCherry::kanMX4</i>
MKY1847	MATa α , <i>his3Δ200</i> , <i>ura3-52</i> , <i>lys2-801</i> , <i>ent1ΔACB(Δ amino acids 294–450)::HIS3MX6</i> , <i>sla2ΔTHATCH-ent1ACB(amino acids 339–450)-2xHA-meGFP::URA3</i> , <i>ABP1-mCherry::kanMX4</i>
MKY1849	MATa α , <i>his3Δ200</i> , <i>ura3-52</i> , <i>lys2-801</i> , <i>ent1ΔACB(Δ amino acids 294–450)::HIS3MX6</i> , <i>sla2ΔTHATCH-ent1ACB(amino acids 339–450)-2xHA-meGFP::URA3</i> , <i>SLA1-mCherry::kanMX4</i>
MKY1850	MATa α , <i>his3Δ200</i> , <i>ura3-52</i> , <i>lys2-801</i> , <i>ent1(T346A, T364A, T395A, T415A, T427A)-2xHA-meGFP::URA3</i> , <i>sla2ΔTHATCH::natNT2</i> , <i>ABP1-mCherry::kanMX4</i>
MKY1851	MATa α , <i>his3Δ200</i> , <i>ura3-52</i> , <i>lys2-801</i> , <i>ent1(T346E, T364E, T395E, T415E, T427E)-2xHA-meGFP::URA3</i> , <i>sla2ΔTHATCH::natNT2</i> , <i>ABP1-mCherry::kanMX4</i>
MKY2065	MATa α , <i>his3Δ200</i> , <i>ura3-52</i> , <i>lys2-801</i> , <i>ent2::hphNT1</i> , <i>tetO₂(ENT1)::kanMX4</i> , <i>tetR::LEU2</i> , <i>ABP1-mCherry::kanMX4</i>
MKY2328	MATa α , <i>his3Δ200</i> , <i>ura3-52</i> , <i>lys2-801</i> , <i>ent1ΔACB(Δ amino acids 294–450)-Lifeact(ABP140 amino acids 1–17)-EGFP::natNT2</i> , <i>sla2ΔTHATCH::hphNT1</i> , <i>ABP1-mCherry::kanMX4</i>
MKY2329	MATa α , <i>his3Δ200</i> , <i>ura3-52</i> , <i>lys2-801</i> , <i>ent1ΔACB(Δ amino acids 294–450)-Lifeact(ABP140 amino acids 1–17)-EGFP::natNT2</i> , <i>sla2ΔTHATCH::hphNT1</i> , <i>SLA1-mCherry::kanMX4</i>

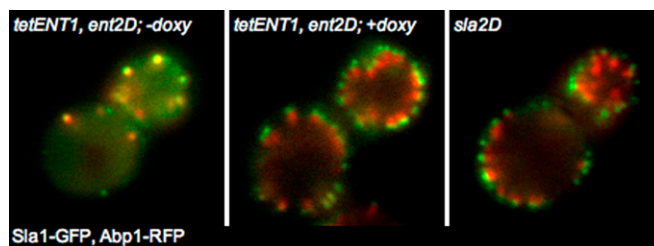
Table S2. Plasmids used in this study

Name	Construction
pRS416- <i>P</i> _{ENT1} -2xHA-meGFP	387 bp of the 5' UTR of the <i>ENT1</i> gene were PCR amplified from genomic DNA and cloned into the SacI-BamHI sites of pRS416ADH-6His-meGFP (a gift of M. Knop, Center for Molecular Biology of the University of Heidelberg, Heidelberg) to generate the plasmid for the expression of <i>ENT1</i> fragments as C-terminal 2xHA-meGFP fusion proteins under the control of the <i>ENT1</i> promoter (the Ascl-Xmal sites and 2xHA tag sequence were added upstream of meGFP sequence).
pRS416- <i>P</i> _{ENT2} -2xHA-meGFP	422 bp of the 5' UTR of the <i>ENT2</i> gene were PCR amplified and cloned similarly to pRS416- <i>P</i> _{ENT1} -2xHA-meGFP.
pRS416-Ent1-ENTH-2xHA-meGFP	The sequence coding for ENTH domain of Ent1 (amino acids 1–154) was PCR amplified from genomic DNA and cloned into the Ascl-Xmal sites of pRS416- <i>P</i> _{ENT1} -2xHA-meGFP.
pRS416-Ent2-ENTH-2xHA-meGFP	The sequence coding for ENTH domain of Ent2 (amino acids 1–156) was PCR amplified from genomic DNA and cloned into the Ascl-Xmal sites of pRS416- <i>P</i> _{ENT2} -2xHA-meGFP.
pRS416-Ent1-ENTH T104A-2xHA-meGFP	The sequence coding for ENTH domain of Ent1 was PCR amplified from pRS416-Ent1-ENTH-2xHA-meGFP with mutagenic primers using a fusion PCR protocol (1). The PCR product with the codon for threonine T104 replaced by the codon for alanine was cloned into the Ascl-Xmal sites of pRS416- <i>P</i> _{ENT1} -2xHA-meGFP.
pRS416-Ent2-ENTH T104A-2xHA-meGFP	The sequence coding for ENTH domain of Ent2 was PCR amplified from pRS416-Ent2-ENTH-2xHA-meGFP with mutagenic primers using a fusion PCR protocol. The PCR product with the codon for threonine T104 replaced by the codon for alanine was cloned into the Ascl-Xmal sites of pRS416- <i>P</i> _{ENT2} -2xHA-meGFP.
pRS416-Ent1(140–454)-2xHA-meGFP	The sequence coding for amino acids 140–454 of Ent1 was PCR amplified from genomic DNA and cloned into the Ascl-Xmal sites of pRS416- <i>P</i> _{ENT1} -2xHA-meGFP. To preserve the functionality of the C-terminal clathrin-binding motif of Ent1 in the fusion protein, a codon for Asp was added at the 3' end of the <i>ENT1</i> sequence.
pRS416-Ent2(155–613)-2xHA-meGFP	The sequence coding for amino acids 155–613 of Ent2 was PCR amplified from genomic DNA and cloned into the Ascl-Xmal sites of pRS416- <i>P</i> _{ENT2} -2xHA-meGFP. To preserve the functionality of the C-terminal clathrin-binding motif of Ent2 in the fusion protein, a codon for Asp was added at the 3' end of the <i>ENT2</i> sequence.
pRS416-Ent1(140–294)-2xHA-meGFP	The sequence coding for amino acids 140–294 of Ent1 was PCR amplified from genomic DNA and cloned into the Ascl-Xmal sites of pRS416- <i>P</i> _{ENT1} -2xHA-meGFP.
pRS416-Ent1(294–454)-2xHA-meGFP	The sequence coding for amino acids 294–454 of Ent1 was PCR amplified from genomic DNA and cloned into the Ascl-Xmal sites of pRS416- <i>P</i> _{ENT1} -2xHA-meGFP.
pRS416-Ent1(338–405)-2xHA-meGFP	The sequence coding for amino acids 338–405 of Ent1 was PCR amplified from genomic DNA and cloned into the Ascl-Xmal sites of pRS416- <i>P</i> _{ENT1} -2xHA-meGFP.
pRS416-Ent2(421–609)-2xHA-meGFP	The sequence coding for amino acids 421–609 of Ent2 was PCR amplified from genomic DNA and cloned into the Ascl-Xmal sites of pRS416- <i>P</i> _{ENT2} -2xHA-meGFP.
pRS416-Ent1(294–454)-2xHA	To delete the sequence coding for meGFP in pRS416-Ent1(294-454)-2xHA-meGFP, plasmid was cut with BamHI-XhoI, blunted with Mung Bean nuclease, and religated.
pRS416-Ent1(338–405)-2xHA	To delete the sequence coding for meGFP in pRS416-Ent1(338-405)-2xHA-meGFP, plasmid was cut with BamHI-XhoI, blunted with Mung Bean nuclease, and religated.
pRS416-Ent1(294–454) T→A-2xHA-meGFP	The sequence coding for amino acids 294–454 of Ent1 was amplified from pRS416-Ent1(294-454)-2xHA-meGFP with mutagenic primers using a fusion PCR protocol (1). The PCR product with the codons for threonines T346, T364, T395, T415, and T427 replaced by codons for alanines was cloned into the Ascl-Xmal sites of pRS416- <i>P</i> _{ENT1} -2xHA-meGFP.
pRS416-Ent1(294–454) T→E-2xHA-meGFP	The sequence coding for amino acids 294–454 of Ent1 was amplified from pRS416-Ent1(294-454)-2xHA-meGFP with the mutagenic primers using a fusion PCR protocol. The PCR product with the codons for threonines T346, T364, T395, T415, T427 exchanged to codons for glutamates was cloned into the Ascl-Xmal sites of pRS416- <i>P</i> _{ENT1} -2xHA-meGFP.
pETM30-Ent1-ENTH	Codon-optimized sequence coding for ENTH domain of Ent1 (amino acids 1–154) was synthesized (Entelechon, Germany) and cloned into the NcoI-XhoI sites of pETM30 (provided by European Molecular Biology Laboratory Protein Expression and Purification Core Facility).

Table S2. Cont.

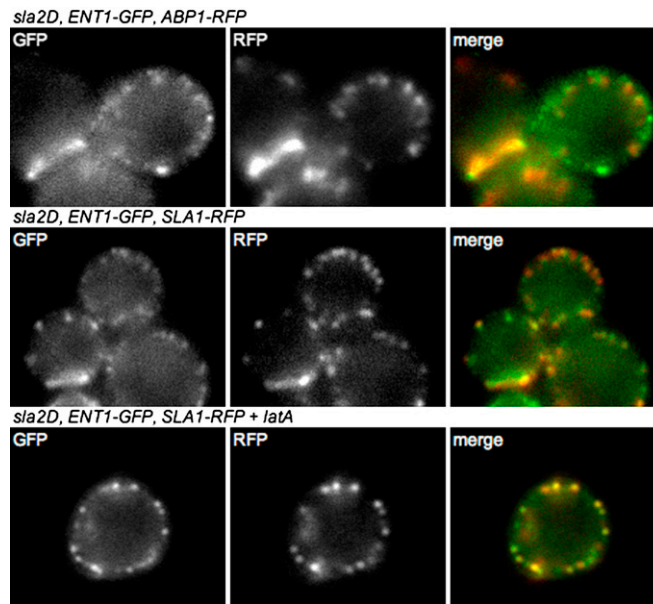
Name	Construction
pETM30-Ent1-ENTH T104A	The sequence coding for Ent1-ENTH was amplified from pETM30-Ent1-ENTH with mutagenic primers using a fusion PCR protocol. The PCR product with the codon for threonine T104 exchanged to codon for alanine was cloned into the NcoI-XhoI sites of pETM30.
pETM30-Sla2-ANTH	Codon-optimized sequence coding for ANTH domain of Sla2 (amino acids 1–286) was synthesized (Entelechon, Germany) and cloned into the NcoI-XhoI sites of pETM30 (provided by European Molecular Biology Laboratory Protein Expression and Purification Core Facility).
pETM30-Ent1(338–405)	The sequence coding for amino acids 338–405 of Ent1 was PCR amplified from genomic DNA and cloned into the BamHI-XhoI sites of pETM30.
pETM30-Ent1(338–405) T→E	The sequence coding for amino acids 338–405 of Ent1 was PCR amplified from pETM30-Ent1(338-405) with the mutagenic primers using a fusion PCR protocol. The PCR product with the codons for threonines T346, T364, T395 exchanged to codons for glutamates was cloned into the BamHI-XhoI sites of pETM30.

1. Ho SN, Hunt HD, Horton RM, Pullen JK, Pease LR (1989) Site-directed mutagenesis by overlap extension using the PCR. *Gene* 77:51–59.



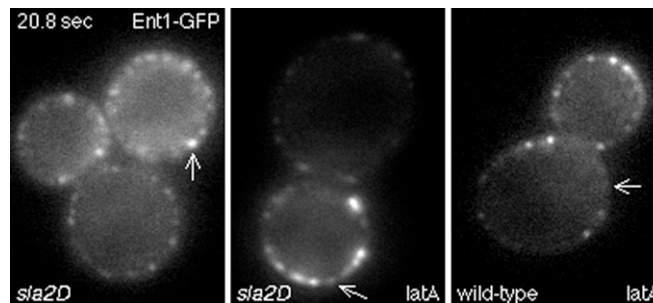
Movie S1. The uncoupling phenotype in epsin-depleted and *sla2Δ* cells. Two-color movie shows Sla1-GFP (green) and Abp1-RFP (red) in an epsin-depleted (*tetENT1, ent2Δ*) strain cultivated for 7 h with 25 μg/mL of doxycycline (+doxy) or without doxycycline (– doxy) and in an *sla2Δ* strain. The interval between frames is 3 s. The total time of acquisition was 240 s.

[Movie S1](#)



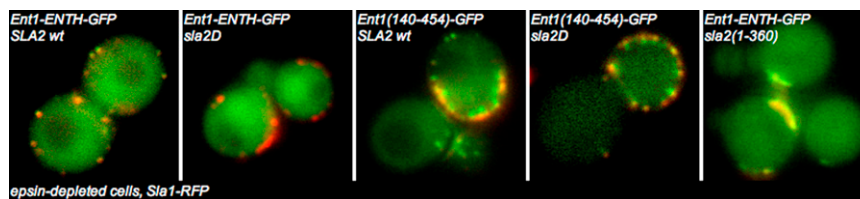
Movie S2. Behavior of Ent1-GFP, Sla1-RFP and Abp1-RFP at endocytic sites of *sla2Δ* cells. Ent1-GFP and Abp1-RFP in *sla2Δ* cells (Top row), Ent1-GFP and Sla1-RFP in *sla2Δ* cells (Middle row), and Ent1-GFP and Sla1-RFP in latA-treated *sla2Δ* cells (Bottom row) are shown. The interval between frames is 2 s. The total time of acquisition was 120 s.

[Movie S2](#)



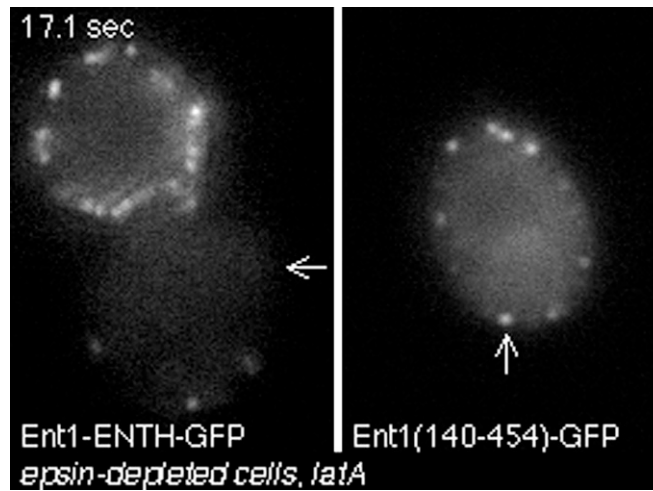
Movie S3. FRAP of Ent1-GFP in *sla2Δ* cells, latA-treated *sla2Δ* cells, and latA-treated wild-type cells. The time of each frame related to the bleaching time (time 0) is shown in the upper left corner. The arrows mark the bleached endocytic patches.

[Movie S3](#)



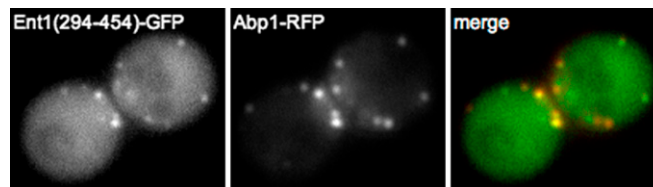
Movie S4. Localization of Ent1-ENTH-GFP and Ent1(140-454)-GFP in epsin-depleted cells expressing variants of the SLA2 gene. Two-color movie shows epsin-depleted cells expressing the indicated Sla2 mutants and Sla1-RFP (red) together with Ent1-ENTH-GFP or Ent1(140-454)-GFP (green) expressed by the endogenous promoter from a CEN plasmid. The interval between frames is 3 s. The total time of acquisition was 90 s.

[Movie S4](#)



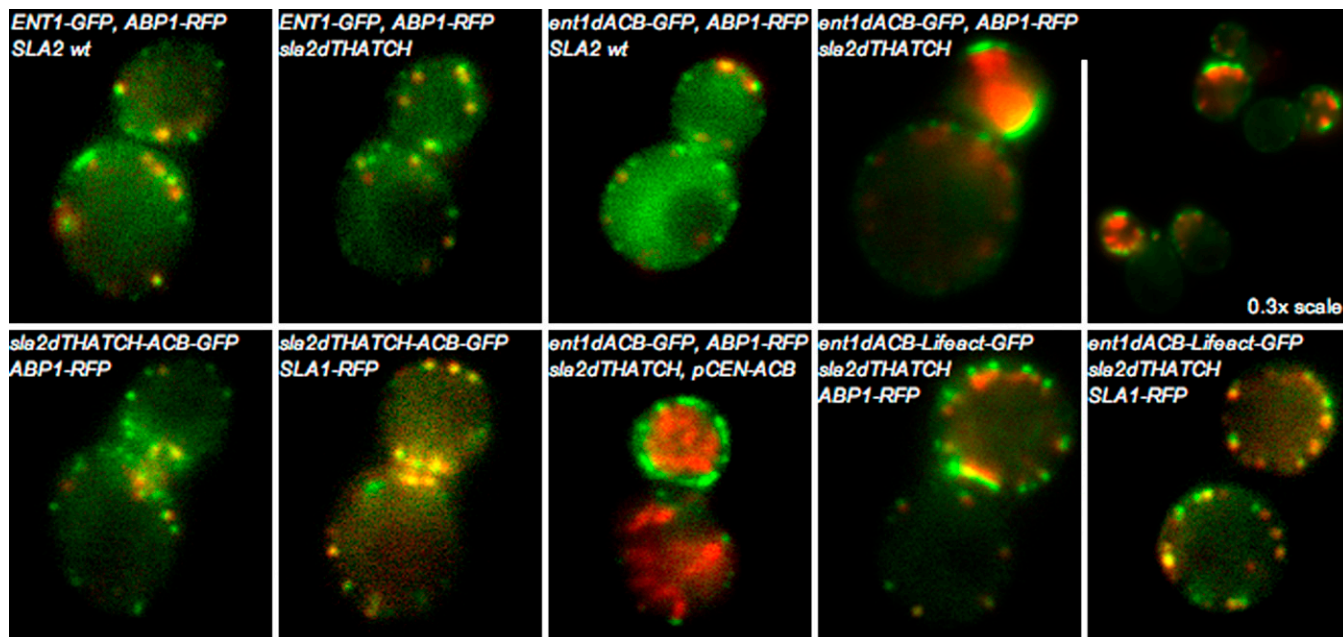
Movie S5. FRAP of Ent1-ENTH-GFP and Ent1(140-454)-GFP in latA-treated epsin-depleted cells. The time of each frame related to the bleaching time (time 0) is shown in the upper left corner. The arrows mark the bleached endocytic patches.

[Movie S5](#)



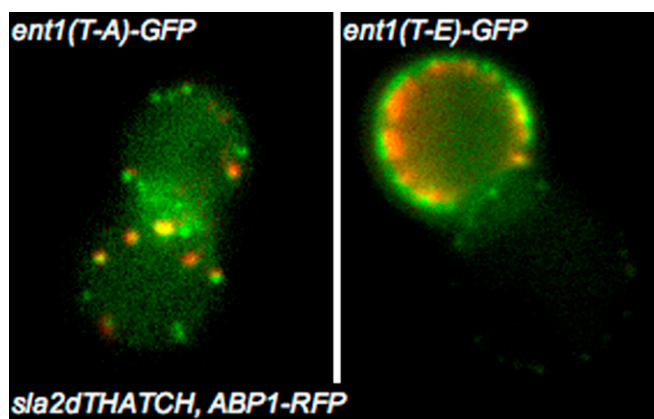
Movie S6. Colocalization of Ent1(294-454)-GFP with Abp1-RFP in wild-type cells. The dynamics of Ent1(294-454)-GFP expressed by the endogenous promoter from a *CEN* plasmid and Abp1-RFP at endocytic sites of an otherwise wild-type strain is shown. The interval between frames is 2 s. The total time of acquisition was 120 s.

[Movie S6](#)



Movie S7. The Ent1 ACB and Sla2 THATCH domains bind redundantly to the actin cytoskeleton. (*Upper row*) Two-color movie shows strains expressing Abp1-RFP (red) together with Ent1-GFP or Ent1 Δ ACB-GFP (green) in a wild-type *SLA2* or *sla2* Δ THATCH strain, respectively. A field with more cells expressing Ent1 Δ ACB-GFP, Sla2 Δ THATCH and Abp1-RFP is shown in the far right panel in 0.3 \times scale in comparison with other panels. (*Lower Row, first and the second panels*) Two-color movie shows an *ent1* Δ ACB strain expressing the Sla2 Δ THATCH-ACB chimeric protein as a GFP fusion (green) together with Abp1-RFP (first panel; red) or Sla1-RFP (second panel; red), respectively. (*Lower Row, third panel*) Two-color movie of an *ent1* Δ ACB-GFP, *sla2* Δ THATCH, *ABP1-RFP* strain expressing the ACB domain-containing Ent1(294-454) fragment by the endogenous promoter from a *CEN* plasmid. (*Lower Row, fourth and fifth panels*) Two-color movie shows an *sla2* Δ THATCH strain expressing the Ent1 Δ ACB-Lifeact chimeric protein as a GFP fusion (green) together with Abp1-RFP (fourth panel; red) or Sla1-RFP (fifth panel; red), respectively. For all movies the interval between frames is 3 s. The total time of acquisition was 180 s.

[Movie S7](#)



Movie S8. Phenotypes of the Ent1(T-A) and Ent1(T-E) phosphomutants in *sla2* Δ THATCH cells. Two-color movie shows an *sla2* Δ THATCH strain expressing Abp1-RFP (red) together with Ent1(T-A)-GFP or Ent1(T-E)-GFP (green). The interval between frames is 3 s. The total time of acquisition was 180 s.

[Movie S8](#)